Design and evaluation of gas transport through a zeolite membrane on an alumina support.

SHEHU, H., OKON, E., ORAKWE, I. and GOBINA, E.

2018

Chapter 3

Design and Evaluation of Gas Transport through a Zeolite Membrane on an Alumina Support

Habiba Shehu, Edidiong Okon,
Ifeyinwa Orakwe and Edward Gobina

Additional information is available at the end of the chapter

http://dx.doi.org/10.5772/intechopen.75545

Abstract

This chapter details the synthesis and applications of zeolite membranes (gas separation and zeolite membrane reactors). Gas separation is still not carried out at industrial level for zeolite membranes. Related areas, such as the possibility of incorporating a zeolite membrane in a reactor for possible catalytic action of the zeolite particles and scale-up issues are also discussed. The basic concept of mass transport through the zeolite layer has been presented. Zeolites can enhance the selectivity of methane more which can lead to the reduction of greenhouse gases in the atmosphere.

Keywords: zeolite membranes, greenhouse gases, catalytic membrane reactor and gas separations

1. Introduction

Volatile organic compounds vapourises easily to the atmosphere due to their high vapour pressure. Light hydrocarbons like methane, ethane and propane are considered as VOCs [1]. As stated previously, methane has a global warming potential (GWP) 21 times greater than CO_2. **Table 1** shows the GWP for methane, carbon dioxide and several hydrocarbon gases, while **Figure 1(a)** shows the percentage of the GHGs emitted.

Worldwide emissions of GHG can be presented according to the economic activities that lead to their production, as indicated in **Figure 1(b)** [2]. These include,

Components	GWP
Methane	21
Ethane	5.5
Propane	3.3
Butane	4
Carbon dioxide	1

Table 1. Global warming potentials for several VOC components [1].

- Electricity and heat production: This sector accounts for the highest percentage of GHG emissions at 25% (in 2010), as reported by the United States Environmental Protection Agency (EPA). Hence, the burning of fossil fuels (*i.e.* coal, natural gas and oil) for electricity and heat generation are the main activities that contribute to the global increase of GHG.
- Industry: GHG emissions from industry primarily involve onsite burning of fossil fuels for energy. This area incorporates emissions from mineral transformation processes which are not as a result of energy consumption, chemical, metallurgical and emissions from activities of waste management. This sector accounts for 21% of GHG (**Figure 1(b)**).
- Agriculture, forestry and other land uses: GHG emissions from this sector originate primarily from deforestation and planting of trees. This value does not include carbon dioxide removed from the atmosphere by dead organic matter, carbon sequestering in biomass and soils, which reduces about 20% of emissions from this sector.

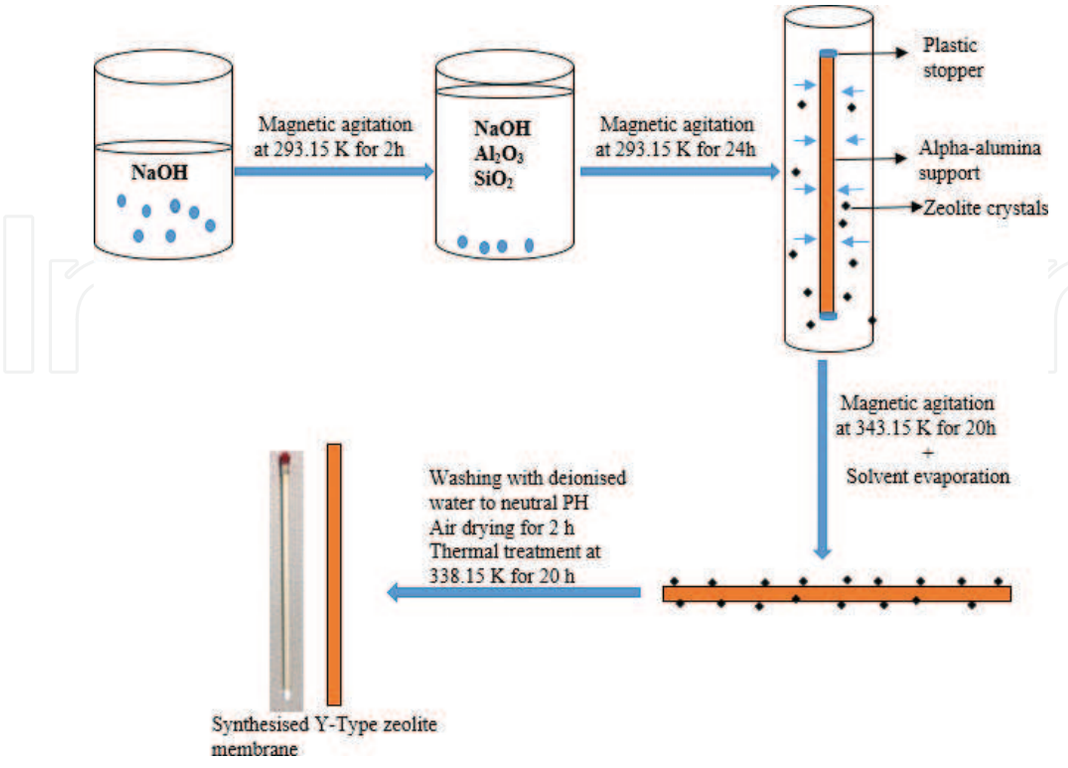

Figure 1. Schematic of the solid-state crystallisation route for y-type zeolite synthesis.

- Transportation: GHG emissions from transportation include the use of fossil fuels that are burned for rail, road, water and air transportation. Petroleum-based fuels account for about 96% of global transportation energy; this is mainly from diesel and gasoline.
- Buildings: This area accounts for the smallest GHG emissions (6%) and the emissions mainly arise from onsite energy generation and burning fuels for heat in buildings or cooking in homes.
- Other Energy: Other sources of GHG emissions come from the Energy sector which are not directly associated with electricity or heat production. For example, oil and gas extraction, refining, processing, and transportation.

The work carried out in this research considers the economic sector of GHG emissions namely, transportation and storage of crude oil as well as natural gas processes. A technology to separate the major GHGs methane and carbon dioxide and further utilise them in valuable feed stock has been explored using a y-type zeolite membrane.

Zeolites are natural or synthetic compounds that are composed of hydrated alumina-silica structures of alkaline and alkaline-earth metals. They have attracted increased interest because of their similar pore size on the molecular scale, which enables the separation of liquid and gaseous mixtures in a continuous way [3]. Zeolites have good chemical and thermal stability. As such, they can be used for high temperature processes and for processes that employ organic solvents. In addition, zeolite materials exhibit intrinsic catalytic property, which promotes the use of zeolite membranes as catalytic membrane reactors (CMRs).

In the previous two decades, enormous progress has been made on zeolite membrane synthesis. However, only 20 out of approximately 170 zeolite structures are used for the preparation of a membrane [4]. The high cost and poor reproducibility of the synthesis hinders the application of the zeolite membranes on a large industrial scale [5, 6]. Zeolite frameworks are made of silicon oxides and aluminium oxides. Moreover, the silicon and aluminium atom centres have a tetrahedral shape, which are linked to each other by bridging oxygen atoms. The strong acidity and uniformity of the micropores (less than 2 nm in diameter), together with a unique crystal structure ensures that zeolites have a high selectivity for separation based on the shape or chemical configuration of molecules in different chemical reactions. For example, alkylation, aromatisation, cracking, pyrolysis, and hydrodesulphurisation.

In comparison to natural zeolites, synthetic zeolites (*i.e.* X, Y and A) are often more applicable in membrane technology due to their uniform particle size and high purity. In addition, they can be designed to separate hydrocarbons. Van Bekkum et al. [7] have previously prepared an MFI-type zeolite membrane on a porous stainless steel disk. These exhibited a high permselectivity for *n*-butane (*n*-C_4H_{10}) over *i*-butane (*i*-C_4H_{10}) at room temperature. Jia et al. [8] reported on a zeolite membrane that showed a *n*-C_4H_{10}/*i*-C_4H_{10} selectivity of approximately 50 at 20°C. However, the authors reported no data at elevated temperatures. Yan et al. [9] previously prepared an MF membrane on an alumina porous disk. The authors reported a *n*-C_4H_{10}/*i*-C_4H_{10} permselectivity of 6.2 at 108°C and 9.4 at 185°C. Vroon et al. [10] reported the formation of an MFI-type membrane on an alumina support. This was shown to exhibit a *n*-C_4H_{10}/*i*-C_4H_{10} permselectivity of 90 at 25°C and 11 at 200°C. Thus, reproducibility in the membrane formation process is one of the vital factors for the application of zeolite membranes.

In addition, the effect of the supporting substrate on permeation properties of zeolite membranes is critical. Yan et al. [9] reported that the membrane morphology changed for the same porous substrate, under different synthetic conditions. Kusakabe et al. [11] produced an MFI-type zeolite membrane on the exterior surfaces of a porous alumina support tube using a hydrothermal reaction. The authors found no direct relationship between film morphology and permselectivity. The authors also synthesised a Y-type zeolite membrane on a porous α-alumina support tube and carried out single gas permeation test on CO_2, N_2, CH_4, C_2H_6 and SF_6. The authors found that the selectivity of CO_2/CH_4 through the membrane was higher at permeation temperatures that are lower, and tends to decrease with increases in temperature.

1.1. Mass transfer through a zeolite membrane

The process of mass transport through a zeolite layer arises via the five steps listed below [12, 13]:

1. Adsorption of the substance on the outer surface of the membrane.
2. Mass transport from the outer surface into the zeolite pore.
3. Diffusion of intra-crystalline zeolite.
4. Mass transport out of the zeolite pores to the external surface.
5. Desorption from the outer surface to the bulk.

Adsorption and desorption of species from the outer surface of a zeolite layer depends on the permeation conditions (*i.e.* temperature and pressure), type of crystalline material and the nature of the chemical species. Steps 2, 3 and 4 are usually activated processes [14].

Intra-crystalline permeation through a zeolite membrane can be described using several approaches [15]. The Fickian approach considers the concentration gradient as the driving force in a zeolite membrane. Alternatively, the gradient of the thermodynamic potential is the driving force in the Maxwell-Stefan (MS) approach. The MS approach allows for the approximation of the flux through the membrane for multicomponent gas mixtures by using information about single gas permeations [16]. The Fickian approach can be applied for permeation of single gas components through a zeolite membrane at a wide range of temperatures. Moreover, it can be assumed that the total flux N is the combination of the surface flux N_s, which takes place at low to medium temperatures, and the activated gaseous flux N_g, which is prevalent at high temperatures [13–15]. This is given by Eq. (1):

$$N = N_s + N_g \tag{1}$$

Fick's diffusivity D_s is given by Eq. 32:

$$D_s = D_o \Gamma \tag{2}$$

http://dx.doi.org/10.5772/intechopen.75545

where D_o is the intrinsic or corrected diffusivity and Γ is the thermodynamic correction factor, which is expressed as:

$$\Gamma = \frac{dln\, p_i}{dln\, c_i} \tag{3}$$

where P_i and c_i are the pressure and concentration of component i.

The transport diffusivity is dependent on the temperature. This is more apparent at higher temperature. The assumption of an Arrhenius type dependence on temperature can be assumed [16], giving by:

$$D_o = \frac{D_g}{RT}\left(\frac{dp}{dz}\right) \tag{4}$$

The dependence on temperature will be affected by the adsorption of the component on the zeolite as well as the operating conditions. Moreover, the adsorption phenomena can be negligible at elevated temperatures. Under these conditions molecules can be considered to be in a quasi-gaseous state in the zeolite framework. This is referred to as activated Knudsen diffusion or gas translational diffusion. When this occurs, the flux is expressed as:

$$N_g = -\frac{D_g\, dp}{RTdz} \tag{5}$$

where dp/dz is the pressure gradient and also the permeance driving force. The diffusion coefficient that is dependent on the gas molecular velocity is given by:

$$D_g = d_p\, u_m\, e^{-E_r/RT} \tag{6}$$

where d_p is the pore diameter and u_m is the average velocity.

For ideal gases, kinetic theory can be used to calculate the molecular velocity given by Eq. (7):

$$u_m = \sqrt{\frac{8RT}{\pi M}} \tag{7}$$

From the equations above, it is clear that gas transport through a zeolite membrane is dependent on the adsorptive interaction between the permeating gas molecule and the zeolite. Moreover, the permeating flux is meant to increase with an increase in temperature. This is true for a defect free zeolite membrane. However, Knudsen and viscous flow can contribute to the overall flux and will strongly influence the expected temperature dependence when defects are present [16].

The ramification of predicting the mass transport and separation through synthesised zeolite membranes, where defects of inter-crystalline nature also need to be considered, is evident even though a simple approach has been used. High selectivity separations can be achieved by using nearly perfect zeolite membranes. In addition to high permselectivity, zeolite membranes should exhibit a high permeation flux in order to be suitable for industrial scale

applications. This can be achieved with minimal membrane thickness. Regrettably, decreasing the membrane thickness results in negative effect of inter-crystalline defects on permselectivity can be limiting. The thickness of a zeolite layer is dependent on the synthesis routes, conditions and on the number of depositions. For example, White et al. [15] obtained a ZSM-5 membrane by direct *in situ* crystallisation with a two-step deposition and showed a thickness between 30 and 40 μm. At laboratory level, zeolite membranes with a thickness of a few microns can be obtained with sufficient quality. Currently there are ongoing investigations to find a way to avoid, reduce or eliminate the presence of inter-crystalline defects, which, aside from poor synthesis reproducibility, are the main obstacle to the widespread industrial application of zeolite membrane. Moreover, if mixtures of gas and vapour having high molecular masses, or liquid mixtures of two species with different volatility and surface tension, are considered, the separation factors and permeation fluxes can be very interesting. However, these separations cannot be extrapolated from the permeances of the pure gases.

1.2. Membrane transport mechanism

In order to understand the fundamentals of membrane gas separation, a brief introduction to some laws and processes commonly employed is required.

1.2.1. Graham's law (Thomas Graham in 1848)

Graham's law states that the rate of diffusion of a gas is inversely proportional to the square root of its molecular weight. This can be written as,

$$\frac{Rate_a}{Rate_b} = (M_b/M_a)^{1/2} \tag{8}$$

where $Rate_a$ is the rate of diffusion of the first gas (volume or number of moles per unit time), $Rate_b$ is the rate of diffusion for the second gas, and M_a and M_b are the molar masses of gases a and b in g mol^{-1}.

1.2.2. Fick's first law

Fick's first law relates the diffusive flux to the concentration under the assumption of steady state. It postulates that the flux goes from regions of high concentration to regions of low concentration. The law fundamentally describes diffusion of species and was enunciated by Adolph E. Fick in 1855, who noted a similarity between diffusion of solutes and Fourier's law describing the flow of heat in solids. Fick's law was theoretically deduced in 1860 by James C. Maxwell from the kinetic theory of gases. The derivation of Fick's law includes the following assumptions: (1) statistical laws apply, (2) the average duration of a collision is short compared to the average time between collisions, a condition pertaining to dilute solutions, (3) particles move independently, (4) classical mechanics can be used to describe molecular collisions, (5) energy, momentum and mass are conserved in every collision, and (6) the diffusing solute particles are much larger than the solvent molecules of the liquid.

The separation of gases in membranes is possible due to the difference in the movement of the different species through the membrane. For membranes having large pore sizes of 0.1–10 μm,

http://dx.doi.org/10.5772/intechopen.75545

the gases permeate via convective flow and there is no separation of the gases observed. For mesoporous membranes, separation is based on the collision amongst the molecule and hence molecular diffusion is dominant and the mean free path (which is the average distance travelled by a gas molecule between collisions with another gas molecule) of the gas molecules is greater than the pore size. The diffusion here is governed by Knudsen mechanism and it follows from the kinetic theory of gases that the rate of transport of any gas is inversely proportional to the square root of its molecular weight, which coincides with Graham's law of diffusion [16]. However, for a microporous membrane with pore size less than 2 nm, separation of gases is based mostly on molecular sieving. The transport mechanism in these type of membranes is often rather complex and involves surface diffusion that occurs when the permeating species exhibit a strong affinity for the membrane surface, thus adsorbing on the walls of the pores [16].

The permeation of gases through a membrane is dependent on both the diffusion and the concentration gradient of the species along the membrane. The selective transport of a gas molecule through a membrane is often associated with the pressure, temperature, electric potential and concentration gradient. The permeability and selectivity are some of the parameters that are used to determine the performance of a membrane. The permeance, P (mol m^{-2} s^{-1} Pa^{-1}), represents the proportionality coefficient with a flux at steady state for a gas passing through a membrane and is defined by Eq. 9:

$$P = \frac{Q}{A.\Delta p} \tag{9}$$

where Q is the gas molar gas flow through the membrane (mol s^{-1}), A is the membrane surface area (m) and Δp is the pressure difference across the membrane (Pa). The permeance is a measure of the quantity of a component that permeates through the membrane [16].

The ideal gas selectivity $\alpha_{i,j}$, is the ratio of the permeability coefficients of two different gases as they permeate independently through the membrane is given by Eq. (10):

$$\alpha_{ij} = \frac{P_i}{P_j} \tag{10}$$

where P_i and P_j are the permeance of the single gases through the membrane respectively. The selectivity is the measure of the ability of a membrane to separate two gases and is used to determine the purity of the permeate gas, as well as determine the quantity of product that is lost. The permeability coefficient is related to the diffusivity coefficient, D (m^2 s^{-1}), and the solubility coefficient, S (mol m^3 Pa), for a component, i, [16] and is given by:

$$P_i = D_i.S_i \tag{11}$$

Combining Eqs. (4) and (5), the selectivity of a membrane can be expressed as:

$$\alpha_{ij} = \frac{D_i}{D_j}\frac{S_i}{S_j} \tag{12}$$

For a binary mixture of gases with components i and j, the separation factor SF is given by:

$$SF_{ij} = \frac{(Y_i/Y_j)}{(X_i/X_j)} \tag{13}$$

where Y and X are the percentage concentrations in the permeate and feed end of the membrane. During experiments, the concentration of the gases (X_i and X_j) are fixed while at the permeate side Y_i and Y_j are determined using gas chromatography (GC).

1.3. Knudsen diffusion

Knudsen diffusion arises from differences in the molecular weights of components to be separated. This proceeds at a speed that is inversely proportional to the square root of the molecular weight of the component. Separation by Knudsen diffusion requires that the pore diameter of the membrane to be smaller than the mean free path of the components. Generally, diffusion of gases through porous membranes is dependent on the type of collisions that occur. At low concentrations, where there is predominantly molecule-pore wall collisions then the flow is Knudsen flow. Knudsen flow can be achieved with membranes whose pore size is greater than 4 nm. However, for it to dominate the pore size should be less than 50 nm [17]. In addition, the separation factor for a mixture of binary gases can be estimated from the square root of the ratio of the molecular weights of the gases. This is because gas permeation by Knudsen diffusion varies inversely with the square root of the molecular weights of the gases. Hence an ideal Knudsen separation for a mixture of binary gases is equal to the inverse of the square root of their molecular mass ratio [18]. The transportation equation for Knudsen and viscous flow is given by Eq. (8):

$$J = A\bar{P} + B \tag{14}$$

where $\bar{P}$ is the average pressure across a porous membrane, and A and B are constants relative to the membrane structure, molecular weight and size. According to Eq. (8), A is the constant representing Knudsen flow, while B is the constant representing viscous flow.

1.4. Molecular sieving

The molecular sieving effect in gas separations occurs when the pores of a membrane decrease to the 5 to 10×10^{-10} nm range. If the gases to be separated have different kinetic diameters then the smaller molecules will permeate through the membrane while the larger molecules will be retained. Very high separation can be achieved using this effect [18]. The kinetic diameter of a gas is defined as the intermolecular distance of closest approach for two molecules colliding with zero initial kinetic energy. This is dependent on the molecular shape, size and dipole–dipole interactions [19]. **Table 1** lists the kinetic diameters and molecular weights of several molecules found in natural gas or shuttle tanker exhaust off-gases.

Research in the production of membranes exhibiting these properties has accelerated. Zeolites and ceramic membranes can be modified to achieve these properties. None of the membranes

that have exhibited these properties are known to be commercially available. However, there have been reports indicating the separation of gases that differ in size by just 0.1×10^{-10} nm [17].

1.5. Surface diffusion

Surface diffusion and adsorption is a further mechanism that governs the permeation of gases through membranes that have small pore sizes. When the pore diameter of a membrane is in the range of 50–100 Å then adsorption on the walls of the membrane is observed. It is often noted that the amount of gas that is absorbed on the membrane pore walls is greater than the amount of gas that is not absorbed. The absorbed gas molecules then move by surface diffusion through the membrane with the flow rate obeying Fick's law [17].

1.6. Capillary condensation

Capillary condensation occurs when a porous membrane is in contact with a vapour and the saturation vapour pressure in the pores is different from the saturation vapour pressure of the components [20]. In addition, capillary condensation can occur with increasing gas pressures at temperatures below the critical temperature [21]. Therefore, condensed gas molecules are transported across the membrane pores.

For transport measurements, the molecular fluxes of the gases need to be determined from the uneven concentration profile, which can be used to determine the diffusion coefficient [21].

2. Synthesis of zeolite membrane

Zeolite membranes are normally synthesised on porous alumina supports or stainless steel, because a self-standing zeolite layer is very fragile. The commonly employed procedures used for zeolite membrane synthesis include:

(a) vapour-phase transport.

(b) direct *in situ* crystallisation.

(c) secondary growth.

The structured pores of zeolites, and the ability of zeolites to withstand high temperatures and pressures have made them a unique material for designing membranes. Significant high-profile research is currently being undertaken to develop the synthesis of zeolite membranes. Several of the developed methods for the synthesis of zeolite membranes are reviewed in this section.

2.1. Zeolite films that are free-standing

For molecular sieving applications, this method of preparation is most commonly employed. Teflon and cellulose supports are used as temporary supports for the synthesis [22]. This preparation method has been discontinued because of the fragility of the self-supported membrane.

2.2. Supported zeolite membrane

This is the most commonly synthesised zeolite membrane. An *in-situ* hydrothermal synthesis process is used in the preparation. This method is direct and can produce good membranes. In this process a thin layer of zeolite is crystallised on the pores of the porous support. Various forms of porous inorganic materials can be used as supports. These include titania, alumina, dense glass, carbon and stainless steel. Crystal growth on the support involves the pre-treatment of the support, preparation of zeolite seeds and the seeding. Seeding can be achieved by employing several methods including, rub-coating, dip-coating, vacuum seeding, spin coating and filtration seeding [25].

2.3. Polymeric-zeolite filled membranes

This method involves embedding zeolite crystals in to a polymer matrix [23]. The space between the zeolite crystals is sealed with a gas-tight polymeric structure. A major concern with this preparation method has been pore sizes that are different across the matrix and poor thermal stability.

3. Zeolite membrane characterisation

The morphological of zeolite membranes can be determined using several techniques. In this work, the thickness and morphology of the zeolite membrane have been determined using the SEM. The outer surface and cross-sectional view shows the thickness of the zeolite layer on the support and a top view shows the size and shape of the crystals. EDAX has been used to determine the Si/Al ratio as well as the elemental compositions of zeolite membranes.

Fluorescence confocal optical microscopy is a good instrument for the non-destructive analysis of zeolite membranes. The defects of the membrane and the grain boundary network of the zeolite can be observed along the thickness of the membranes and defects may be clearly visualised [24]. N_2 physisorption experiments are typically used to determine the pore volume and porosity of the zeolite powders and membranes. However, this method is difficult to use for supported zeolite membranes, because the supports generally do not fit inside the sample tubes within commercial equipment.

Therefore, in this work, a witness sample of the supported zeolite was used for all characterisation measurements alongside a mortar and pestle that was used to further grind the samples. An alternative method for the determination of porosity in thin films is the porosimetry, which allows analysis of the contribution of micropores and defects to the overall flux through the membrane.

4. Zeolite membrane reactors

Zeolite membrane reactor concept has been developed for equilibrium-limited reactions, products removal and increased reactant conversion rates. They have been used for the in-situ removal of

hydrogen in dehydrogenation reactions. Zeolite membranes having an MFI structure have been used for the conversion of alkanes to olefins. Also, isobutane dehydrogenation has been studied in a membrane reactor combining a platinum/zeolite catalyst and a supported MFI membrane with a tubular configuration [25]. The results provide proof that isobutene yield was found to be about four times greater than the values observed when using a normal reactor. Another study of the dehydrogenation of isobutane revealed that the H_2/isobutane mixture separation factor was close to one at a temperature of about 23°C and increased to 70 at 500°C [22]. These results can be related to the fact that, at reduced temperature, permeation is controlled by adsorption and the permeate is enriched in butane. Diffusion becomes the dominant mechanism when the temperature is increased, this is because the butane is adsorbed less. Furthermore, for the various conditions that were considered experimentally, the membrane reactor showed increased isobutane conversion with respect to the conversion obtained using a normal reactor.

Qi et al. [17] prepared MFI zeolite membranes that contain partial modification of the zeolite channels are able to obtain a high selectivity and permeance during hydrogen separation following a water gas shift reaction at an elevated temperature. Gu et al. [18] have previously modified a zeolite membrane by *in-situ* catalytic cracking of methyl diethoxysilane. The synthesised zeolite membrane showed a H_2/CO_2 permselectivity of 68.3 with a hydrogen permeance of 2.94×10^{-7} mol m^{-2} s^{-1} Pa^{-1}. The membrane also presented a high stability in the temperature range 400–550°C. Moreover, the membrane reactor achieved a carbon monoxide conversion of 81.7% at 550°C. This is higher than that obtained using a PBR.

Fischer–Tropsch synthesis (FTS) allows for the synthesis of liquid hydrocarbons from various feedstocks, including coal and natural gas. The removal of water from this synthetic process is important for the following reasons:

- To increase reactor productivity.
- To reduce deactivation of the catalysts.
- To increase the conversion of CO_2 to long-chain hydrocarbons by shifting the equilibrium of the water gas shift reaction [19].

Different hydrophilic zeolite membranes have been used for the selective removal of water from mixtures of H_2 and CO. For example, ZSM-5 and mordenite membranes have been used for the water removal under normal FTS conditions [20]. Mordenite membranes have exhibited increased H_2O fluxes and high permselectivities. An A-type (NaA) zeolite membrane was used to study the permeation of single components of H_2O vapour, CO, H_2, CH_4 and their binary mixtures [21]. The permeance of water vapour in the binary mixture is almost close to the value found in the single gases. However, the permeance of each gas component went down with increasing water content. The results obtained can be used to explain how the adsorbed water molecules in the membrane block the other gas molecules. On raising the temperature, the amount of water adsorbed in the membrane goes slightly lower and the selectivity for water in the binary mixture reduces.

Zeolite membranes act also as distributors to regulate the number of reactants added to a catalyst and thus limit side reactions. The use of membrane reactors is also highly relevant for carrying out oxidative dehydrogenation of alkanes to control the oxygen feed, in order

to limit total combustion that is highly exothermic [23]. Zeolite membranes have also been found to be active for the partial oxidation of propane at 550°C. Another possible application of these membranes is to use them as an active contactor, which is catalytically active but not necessarily permselective [24]. Bernado et al. [24] showed how a catalytic zeolite membrane, with catalytically active particles dispersed in to a thin zeolite layer ensures ultimate contact between reactants and the active site of the catalyst. This reduces by-pass problems that occur in PBR and reduces the pressure drop. The same authors have also studied carbon monoxide selective oxidation (Selox) from hydrogen-rich gas streams using catalytic zeolite membranes.

5. Materials and method

The chemicals, materials and gases used for the experimental work carried out in this chapter are listed as follows:

1. 0.1 M sodium hydroxide (NaOH) supplied by Sigma-Aldrich, UK.
2. Aluminium oxide (Al_2O_3) supplied by Sigma-Aldrich, UK.
3. Deionised Water by Purelab Flex, Elga.
4. Gases (Oxygen, Propane, Methane, Nitrogen, Helium, and Carbon dioxide) supplied by BOC, UK.
5. Silicon dioxide (SiO_2) supplied by Sigma-Aldrich, UK.
6. Y-type Zeolite powder supplied by Sigma-Aldrich, UK

5.1. Zeolite synthesis

A y-type zeolite membrane was synthesised by mixing NaOH, Al_2O_3, SiO_2 and deionised H_2O with a molar ratio of $1SiO_2$:$10Al_2O_3$:14NaOH:$798H_2O$. The NaOH and Al_2O_3 were first dissolved in H_2O. This was followed by the addition of SiO_2 and the mixture was agitated with a magnetic stirrer for 24 h at 293.15 K. 2 g of NaX powder was then added. The γ-alumina support, which consists of 77% alumina and 23% TiO_2 and has a permeable length of 348 mm and an internal and external diameter of 7 and 10 mm respectively was subsequently dipped in the resulting sol and kept under magnetic agitation at 343.15 K for 20 h making sure that it was kept central to the measuring cylinder and also vertical. This allowed the solvent to evaporate and resulted in the deposition of y-type zeolite crystals on the support matrix. The resulting membrane was then washed with deionised H_2O until the pH of the wash water was neutral. The membrane was then air dried for 2 h, using a motor powered rotatory drier at room temperature. It was then subjected to thermally treatment at 338.15 K in an oven for 20 h. The α-alumina support was weighed before and after zeolite deposition to determine the amount of zeolite loaded on the support. A schematic of the crystallisation process is shown in **Figure 1**.

http://dx.doi.org/10.5772/intechopen.75545

6. Results and discussion

6.1. SEM and EDAX observation of solid-state crystallisation deposition on the alumina support

SEM and EDAX have been carried out for different synthesis conditions to reveal the solid-state crystallisation of the zeolite on the support. Zeolite nanoparticles have been found to have an average size of 0.18–3.72 nm (**Figure 2a** and **b**). **Figure 2c** shows the SEM of a fresh support. Following crystallising in a mixture of sodium, aluminium and silicone oxides for 24 h the membrane revealed zeolite nanoparticles embedded in the matrix of the support (**Figure 2d**). These nanoparticles began aggregating in several locations that had unclear boundaries. Moreover, the nanoparticles have a spherical shape and a uniform particle size. The high magnification SEM image (**Figure 2b**) revealed that the nanoparticles could be mesoporous. This has been attributed to the assembly of many nanoparticles of 0.35 to 0.37 nm.

Figure 3 shows an EDAX spectrum for zeolite powder. The EDAX spectrum provides details about the elemental composition of the sample. The results confirm the molecular formula of zeolite to be TO_4, where T is either silicon or/and aluminium. Therefore, the elemental composition indicates that the zeolite powder is made up of tetrahedral units of AlO_4 and SiO_4. The percentage weights of O, Al and Si are 138.04, 34.27 and 37.05 respectively. The percentage weight of Oxygen present is approximately four times that of aluminium and silicon.

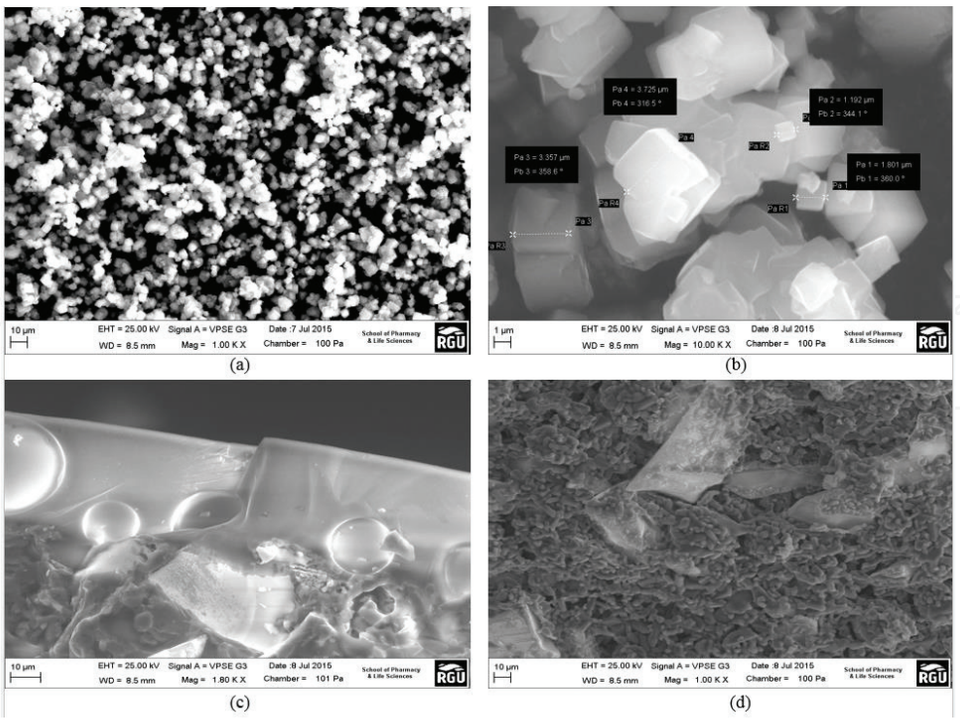

Figure 2. SEM of the zeolite particle samples at (a) before deposition (b) higher magnification before deposition (c) alumina support (d) 24 h crystallisation.

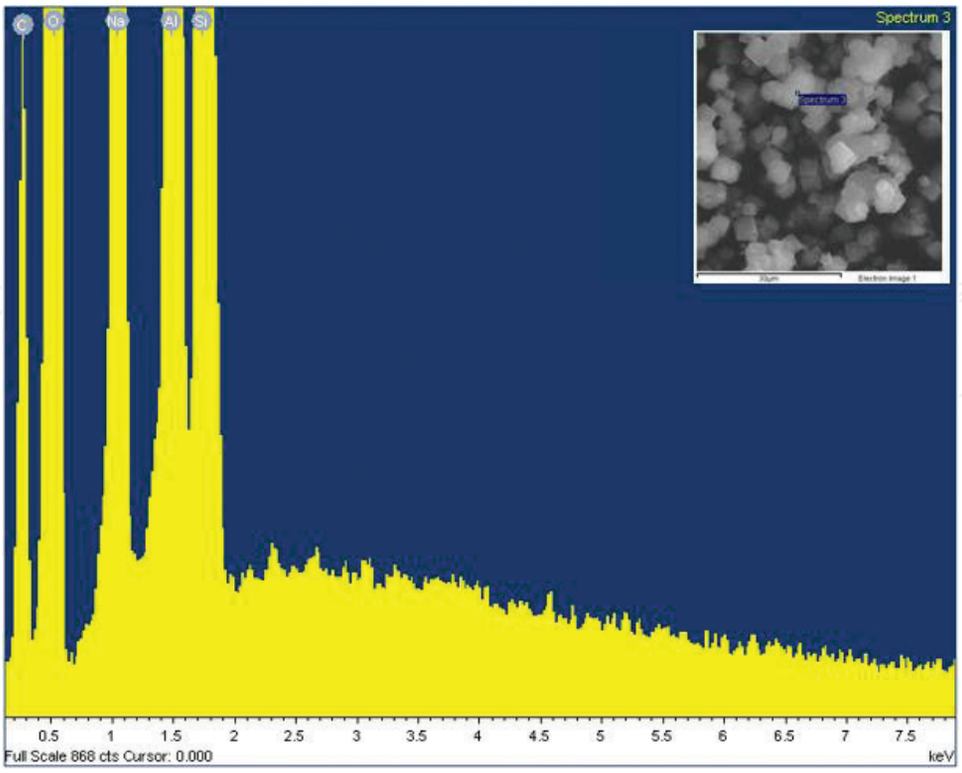

Figure 3. EDAX spectrum of zeolite powder before deposition on alumina support.

In addition, an elemental composition analysis of the y-type zeolite membrane has been determined using EDAX. This is presented in **Figure 4**. The associated data is provided in **Table 2**.

6.2. Nitrogen physisorption measurements

Nitrogen adsorption isotherms of the membrane are shown in **Figure 5**. A summary of the adsorption/desorption data is provided **Table 3**. The pore diameters have been calculated using the Barret-Joyner–Halenda (BJH) model. The BET surface areas for the support and zeolite membranes were found to be 10.69 and 0.106 m^2/g. Zeolites are believed to have large surface areas, however, the synthetic Y-type zeolite has a lower surface area than the support.

6.3. Gas permeation

6.3.1. Effects of temperature on single gas permeation

The single gas permeances for CO_2, N_2, O_2, CH_4 and C_3H_8 have been determined using the gas permeation setup. The permeate stream has been measured at standard temperature and pressure. The flux of the permeate gas has been measured using a volumetric digital flow meter (L min^{-1}). Gas phase conditions have been employed exclusively in the feed and the permeate sides. Subsequently, single gases were fed into the membrane reactor at a pressure range of 0.1 to 1 $\times 10^5$ Pa and at temperatures of 293, 373, 473 and 573 K. Data indicating the change in the flux of the gases through the zeolite membrane, as a function of temperature, are

http://dx.doi.org/10.5772/intechopen.75545

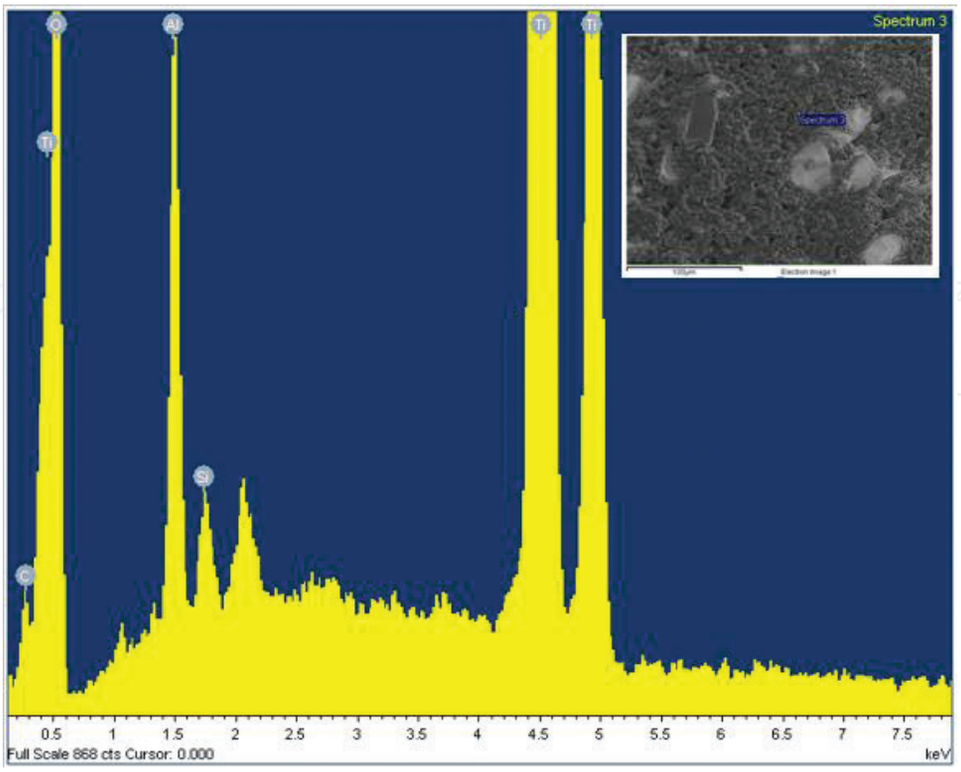

Figure 4. EDAX spectrum of y-type zeolite membrane 24 h after deposition.

presented in **Figures 6** and **7**. The flux is shown to be different for each gas. On increasing the temperature from 273 to 373 K, propane showed an increase of 146% in its flux, whereas there was only a 17% increase for methane. The extent of the effect of temperature is determined by the adsorption of the component on the zeolite. As observed from **Figure 8**, zeolite has a higher affinity towards methane compared to propane. Moreover, the influence of adsorption

Gas	Kinetic diameter ($\times 10^{-10}$ *nm*)	Molecular weight ($g\ mol^{-1}$)
CO_2	3.30	44.01
CH_4	3.80	16.04
N_2	3.64	28.01
CO	3.76	28.01
Ar	3.40	39.95
O_2	3.46	32.00
SO_2	3.60	64.07
NO_2	3.30	46.01
He	2.60	4.00
H_2	2.89	2.02

Table 2. Kinetic diameter and molecular mass of various molecules found in off-gases [19].

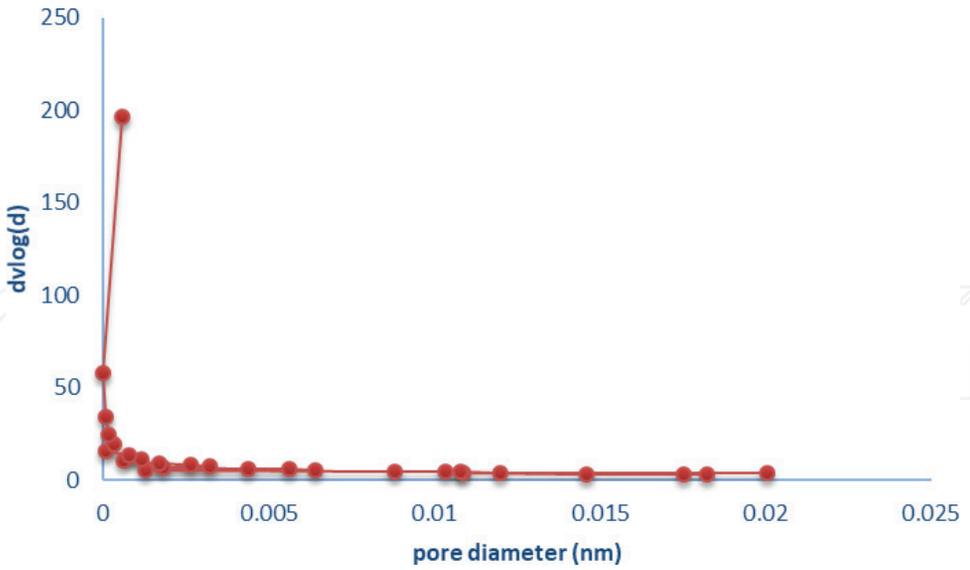

Figure 5. Pore size distribution of zeolite membrane measured by N_2 adsorption/desorption (**Table 4**).

Element	Zeolite powder weight (%)	Synthesised y-type zeolite membrane weight (%)
C	53.72	3.82
Al	34.27	3.11
O	138.04	53.19
Si	37.05	0.50
Ti	—	60.63
Na	30.46	—

Table 3. Elemental composition of the zeolite powder and the synthesised y-type zeolite membrane.

is greater than that of temperature. At elevated temperatures, it is likely that adsorption is negligible and the molecules exist in a quasi-gaseous state in the zeolite framework. Diffusion in this state is referred to as activated Knudsen diffusion or gas translational diffusion.

Selectivity is a measure of the ability of a membrane to separate two gases. It is used to determine the purity of the permeate gas and to determine the quantity of product lost. **Figure 8** shows that C_3H_8/CH_4 selectivity increases from 0.3 at 293 K to 0.9 at 373 K. The higher temperature favours the separation of CH_4 over C_3H_8. However, changes in temperature did not show much significant difference in the separation factors for the CO_2/CH_4 and N_2/CH_4. Moreover, for O_2/CH_4, separation is found to be more favourable at lower temperature (293 K).

6.3.2. Mixed gas permeation using gas chromatograph mass spectrometer (GCMS)

The selectivity of mixed gases was determined by the measure of the concentration of feed and permeate gases through the GCMS using Eq. (7). Details of the GCMS column, carrier

http://dx.doi.org/10.5772/intechopen.75545

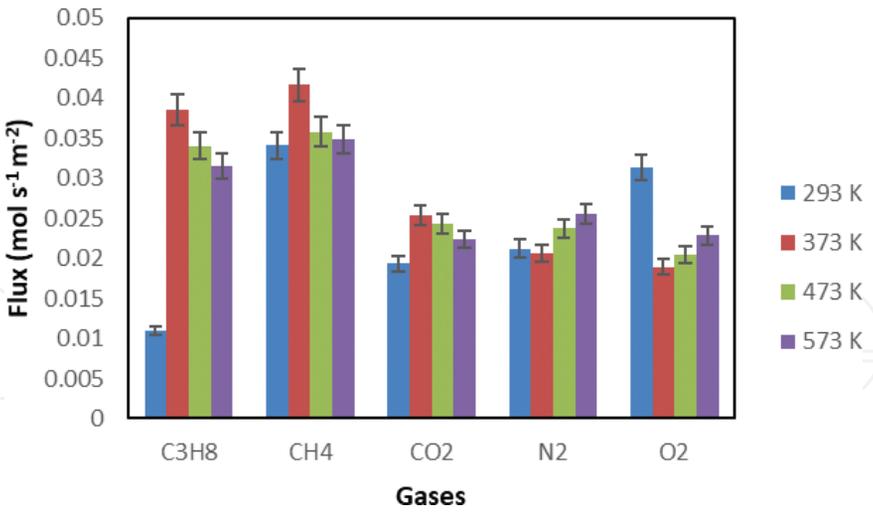

Figure 6. Flux of gases with increase in temperature at 1 × 10^4 pa.

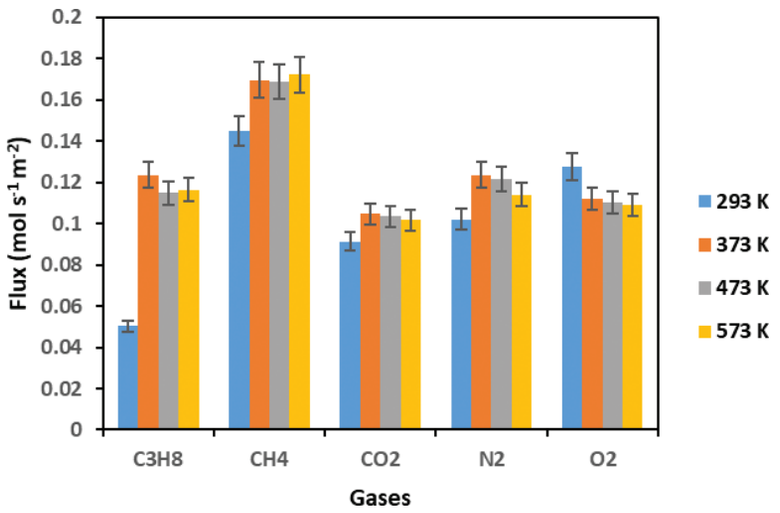

Figure 7. Flux of gases with increase in temperature at 1 × 10^5 Pa.

gas and operating conditions are given in Section 5.6.6. The values calculated for the different binary gas pairs are listed in **Table 5**.

6.3.3. Transport mechanism determination using gas permeation

It has been previously postulated that the linear proportionality of single gas permeance to the inverse of the square root of the molecular weight of the gases indicates that the mode of transport through the membrane is Knudsen diffusion [3]. **Figure 9** plots the relation between the molar gas flux and the inverse of the square root of the gas molecular weight at $1x10^4$ Pa and 293 K. Based on this plot it can be deduced that the gas molar flux is dependent on the molecular weight as previously reported.

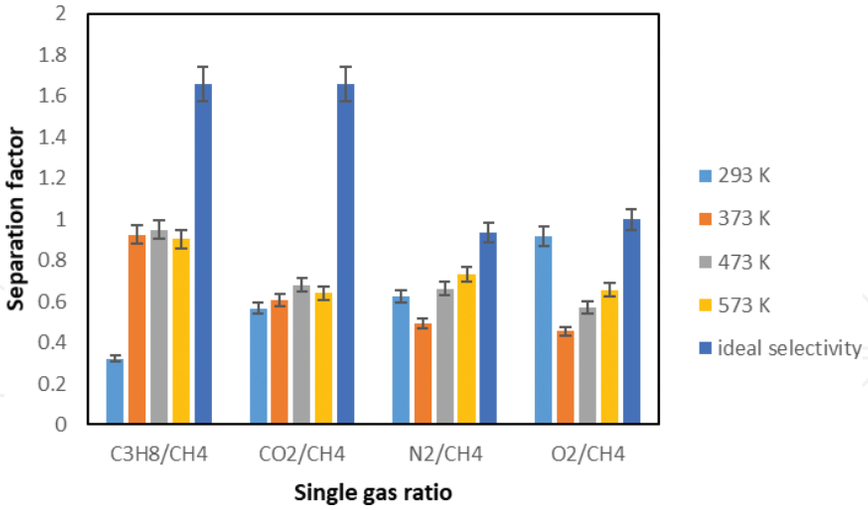

Figure 8. Separation factor of gases with increasing temperature.

Membrane	BET surface area (m^2/g)	Pore diameter (nm)	Pore volume (cm^3/g)
y-type zeolite membrane	0.106	3.139	0.025

Table 4. BET surface area, average pore diameter and pore volume of the membrane.

	CH_4/CO_2 (1.65)	CH_4/N_2 (1.32)	CH_4/C_3H_8 (1.65)
293 k (mixed gases)	1.3	1.8	2.5
293 k (single gases)	1.1	1.6	3.1

Table 5. Selectivity of methane through a zeolite membrane at 293 K.

The order of molecular weight is $CH_4 > O_2 > N_2 > CO_2 > C_3H_8$. However, the R^2 value of 0.807 suggests there is a deviation from Knudsen flow mechanism. CO_2 and C_3H_8 have a similar molecular weight of 44.01 g/mol but the molar flux of CO_2 is greater than that of C_3H_8, this could be explained by molecular sieving flow mechanism, as the kinetic diameter of CO_2 (0.38 nm) is lower than that of C_3H_8 (0.43 nm). **Figure 10** shows the relation between the molar flux and the kinetic diameter of the gases at $1x10^4$ Pa and 293 K. For gases to flow via a molecular sieving mechanism, the smaller molecules must move with a higher molar flux than the larger molecules. There was a deviation to this mechanism, as the order of kinetic diameter is $O_2 > N_2 > CH_4 > CO_2 > C_3H_8$. Moreover, CO_2 and C_3H_8 are observed to permeate through the membrane layer based on their size as C_3H_8 has higher size as compared to CO_2.

http://dx.doi.org/10.5772/intechopen.75545

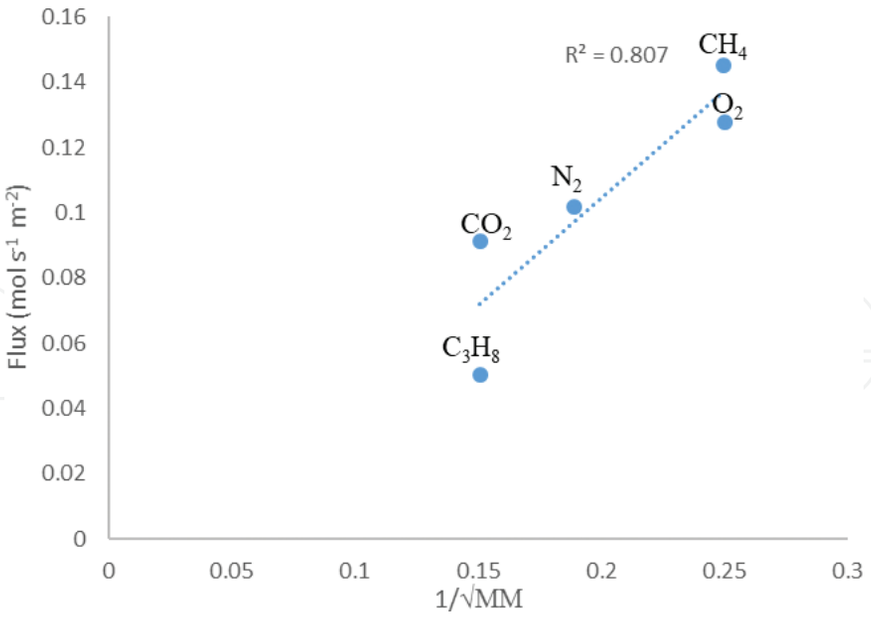

Figure 9. Gas molar flux against the inverse square root of molecular weight.

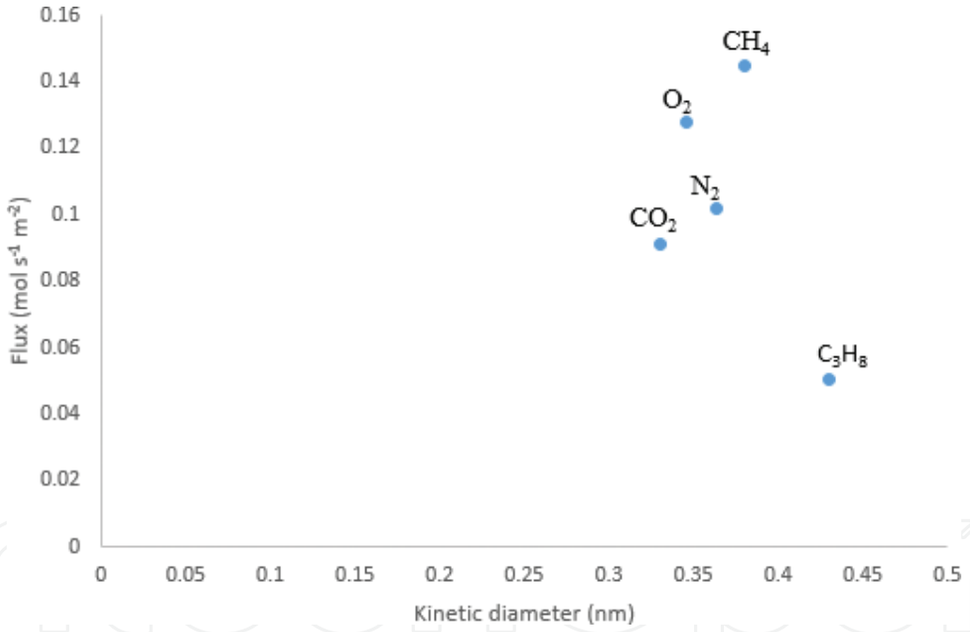

Figure 10. Gas molar flux against kinetic diameter of gases.

7. Conclusions

An evaluation of the performance of y-type zeolite/γ-alumina membrane for natural gas processing has been carried out for separation ability. The transport of gases through the membrane has been shown to be governed by Knudsen diffusion. However, CO_2 and C_3H_8 have been shown to exhibit a molecular sieving mechanism. N_2 adsorption/desorption showed that

at a lower surface area of 0.106 m^2/g, the membrane is more effective at the separation of methane compared to the support. The SEM images revealed asymmetric structure deposition of the zeolite layer. Further studies are planned to demonstrate membrane performance for separating the heavier components of natural gas mixtures that can arise during dew point adjustments, thermal problems during crude oil storage and transportation, and when expanding highly compressed natural gas components.

Author details

Habiba Shehu, Edidiong Okon, Ifeyinwa Orakwe and Edward Gobina*

*Address all correspondence to: e.gobina@rgu.ac.uk

Center for Process Integration and Membrane Technology, Robert Gordon University, Aberdeen, United Kingdom

References

[1] Tamaddoni M, Sotudeh-Gharebagh R, Nario S, Hajihosseinzadeh M, Mostoufi N. Experimental study of the VOC emitted from crude oil tankers. Process Safety and Environmental Protection. 2014;**92**(6):929-937

[2] Ürge-Vorsatz D, Herrero ST, Dubash NK, Lecocq F. Measuring the co-benefits of climate change mitigation. Annual Review of Environment and Resources. 2014;**39**:549-582

[3] Basile A. Handbook of Membrane Reactors: Fundamental Materials Science, Design and Optimisation. Elsevier; 2013

[4] Baerlocher C, McCusker LB, Olson DH. Atlas of Zeolite Framework Types. Elsevier; 2007

[5] McLeary E, Jansen J, Kapteijn F. Zeolite based films, membranes and membrane reactors: Progress and prospects. Microporous and Mesoporous Materials. 2006;**90**(1):198-220

[6] Caro J, Noack M, Kölsch P. Zeolite membranes: From the laboratory scale to technical applications. Adsorption. 2005;**11**(3):215-227

[7] Geus E, Jansen J, Van Bekkum H. Calcination of large MFI-type single crystals: Part 1. Evidence for the occurrence of consecutive growth forms and possible diffusion barriers arising thereof. Zeolites. 1994;**14**(2):82-88

[8] Jia M, Chen B, Noble RD, Falconer JL. Ceramic-zeolite composite membranes and their application for separation of vapor/gas mixtures. Journal of Membrane Science. 1994;**90**(1-2):1-10

[9] Yan Y, Davis ME, Gavalas GR. Preparation of zeolite ZSM-5 membranes by in-situ crystallization on porous. Alpha.-Al_2O_3. Industrial & Engineering Chemistry Research. 1995;**34**(5):1652-1661

[10] Vroon Z, Keizer K, Gilde M, Verweij H, Burggraaf A. Transport properties of alkanes through ceramic thin zeolite MFI membranes. Journal of Membrane Science. 1996;**113**(2):293-300

[11] Kusakabe K, Kuroda T, Murata A, Morooka S. Formation of a Y-type zeolite membrane on a porous α-alumina tube for gas separation. Industrial & Engineering Chemistry Research. 1997;**36**(3):649-655

[12] Burggraaf A. Single gas permeation of thin zeolite (MFI) membranes: Theory and analysis of experimental observations. Journal of Membrane Science. 1999;**155**(1):45-65

[13] Den Exter M, Jansen J, van de Graaf J, Kapteijn F, Moulijn J, Van Bekkum H. Zeolite-based membranes preparation, performance and prospects. Studies in Surface Science and Catalysis. 1996;**102**:413-454

[14] Barrer RM. Porous crystal membranes. Journal of the Chemical Society, Faraday Transactions. 1990;**86**(7):1123-1130

[15] Krishna R, Van Baten J. Describing binary mixture diffusion in carbon nanotubes with the Maxwell-Stefan equations. An investigation using molecular dynamics simulations. Industrial & Engineering Chemistry Research. 2006;**45**(6):2084-2093

[16] Van Dyk L, Miachon S, Lorenzen L, Torres M, Fiaty K, Dalmon J. Comparison of microporous MFI and dense Pd membrane performances in an extractor-type CMR. Catalysis Today. 2003;**82**(1):167-177

[17] Richard W. Baker. Membrane Technology and Applications. 3rd ed. United Kingdom: John Wiley and Sons Ltd; 2012

[18] Gu X, Tang Z, Dong J. On-stream modification of MFI zeolite membranes for enhancing hydrogen separation at high temperature. Microporous and Mesoporous Materials. 2008;**111**(1):441-448

[19] Breck D. Ion exchange reactions in zeolites. Zeolite Molecular Sieves: Structure Chemistry and Use. 1973:529-592

[20] Sidhu PS, Cussler E. Diffusion and capillary flow in track-etched membranes. Journal of Membrane Science. 2001;**182**(1):91-101

[21] Choi J, Do D, Do H. Surface diffusion of adsorbed molecules in porous media: Monolayer, multilayer, and capillary condensation regimes. Industrial & Engineering Chemistry Research. 2001;**40**(19):4005-4031

[22] Illgen U, Schäfer R, Noack M, Kölsch P, Kühnle A, Caro J. Membrane supported catalytic dehydrogenation of iso-butane using an MFI zeolite membrane reactor. Catalysis Communications. 2001;**2**(11):339-345

[23] Tavolaro A, Drioli E. Zeolite membranes. Advanced Materials. 1999;**11**(12):975-996

[24] Lai Z, Bonilla G, Diaz I, Nery JG, Sujaoti K, Amat MA, et al. Microstructural optimization of a zeolite membrane for organic vapor separation. Science (New York, NY). 2003;**300**(5618):456-460

[25] Miachon S, Ciavarella P, Van Dyk L, Kumakiri I, Fiaty K, Schuurman Y, et al. Nanocomposite MFI-alumina membranes via pore-plugging synthesis: Specific transport and separation properties. Journal of Membrane Science. 2007;**298**(1):71-79